



# Seismic behaviors of utility tunnel-soil system: With and without joint connections

Liang Han<sup>a</sup>, Hanlong Liu<sup>a,b</sup>, Wengang Zhang<sup>a,b,d,\*</sup>, Xuanming Ding<sup>a,b,c</sup>,  
Zhixiong Chen<sup>a</sup>, Li Feng<sup>a</sup>, Zhenyu Wang<sup>a</sup>

<sup>a</sup> School of Civil Engineering, Chongqing University, Chongqing 400044, China

<sup>b</sup> Key Laboratory of New Technology for Construction of Cities in Mountain Area, Chongqing University, Chongqing 400044, China

<sup>c</sup> National Joint Engineering Research Center of Geohazards Prevention in the Reservoir Areas, Chongqing University, Chongqing 400044, China

<sup>d</sup> Key Laboratory of Mining Disaster Prevention and Control, Shandong University of Science and Technology, Qingdao 266590, China

Received 19 January 2021; received in revised form 28 July 2021; accepted 5 August 2021

## Abstract

Seismic responses of utility tunnel-soil system were studied via shaking table model tests with considerations of two kinds of double box utility tunnels: with and without joint connections. These two testing utility tunnel models were made of galvanized iron wire and micro-concrete, and the ground was simulated by the dry standard sand through layered tamping treatment. The utility tunnel-soil system was subjected to horizontal vibration in uniaxial direction perpendicular to the longitudinal direction of tunnel model. Via instrumentations of earth pressure gauges, accelerometers and strain gauges, the earth pressure response, acceleration response and bending moment response were measured. The testing results show that the joint connections in the utility tunnel along the longitudinal direction play an important role in determining the characteristic of earth pressure response and bending moment response, whereas the effect of joint connections on acceleration response is less significant. In addition, the partition wall exhibits the consistent acceleration response with the side-wall of double box utility tunnel model under seismic condition. Based on the testing results, it is suggested that the joint connection should be taken reasonably into consideration during design and construction for engineering practice.

**Keywords:** Utility tunnel; Joint connections; Seismic behaviors; Shaking table; Model test

## 1 Introduction

With development of city infrastructure system, land resources are becoming increasingly scarce (Von der Tann et al., 2020; Zhu et al., 2016). Therefore, the utility tunnel is gradually adopted during urbanization to fully utilize the underground space (Wang et al., 2018b; Yang et al., 2019a; Chen et al., 2021) and protect the historic centers (Valdenebro & Gimena 2018), as it provides a practical solution to the complex layout of underground pipelines. On the one hand, many underground pipelines (like high-

voltage cables, water supply pipe, heat pipe, telecommunications cable, and gas pipeline) can be installed in it directly so that workers can maintain these important pipelines conveniently. On the other hand, once the utility tunnel invariably suffers severe damage during natural hazards or other emergencies, the failure of these underground pipelines will further distress the earthquake victims (Sakai et al., 2017). Recently, various studies related to underground utility tunnel have been conducted from the perspective of construction technology (Valdenebro et al., 2019), effect of buried depth (Xu et al., 2018), influence of utility tunnel on adjacent buildings (Tan et al., 2019), settlement control and monitoring (Huang et al., 2018) and economic design (Li et al., 2019), most of which were under the static condition. However, as earthquake is one

\* Corresponding author at: School of Civil Engineering, Chongqing University, Chongqing 400044, China.

E-mail address: [zhangwg@cqu.edu.cn](mailto:zhangwg@cqu.edu.cn) (W. Zhang).

<https://doi.org/10.1016/j.undsp.2021.08.001>

2467-9674/© 2021 Tongji University. Publishing Services by Elsevier B.V. on behalf of KeAi Communications Co. Ltd.

This is an open access article under the CC BY license (<http://creativecommons.org/licenses/by/4.0/>).

of the most serious natural hazards, the seismic performance should not be ignored (Chen et al., 2019b).

In 1995, Kobe earthquake caused a serious damage to a subway station, namely Dakai subway station (Iida et al., 1996). Since then, the seismic performance of underground structure has widely attracted growing attention and lots of relevant researches have been carried out, including field investigation (Iida et al., 1996), seismic response indices (e.g., peak ground acceleration, velocity, and displacement) (Paolucci & Smerzini, 2018), testing method and equipment (Iwatate et al., 2000; Chen et al., 2010; Chen et al., 2013; Wang et al., 2018a; Yan et al., 2018; Yang et al., 2019b; Zhang et al., 2020), the numerical simulations (Chen et al., 2012; Jiang et al., 2010; Chen et al., 2015) and analytical solutions (Davis et al., 2001; Yu et al., 2018) as compiled in Table 1.

Apparently, many countries including China, Japan, Greece, Spain, United States, UK, Korea and so on have conducted relevant researches on seismic performance of underground structures. In terms of the structure type, extensive efforts have been devoted to the seismic behaviors of subway station, tunnel, subway structure, underground pipeline and utility tunnel since 1995, whereas the utility tunnel could not be paid attention before 2010. In terms of research method, shaking table model test and numerical simulation are mostly applied to the study of seismic behaviors of underground structure-soil system in the recent years because of the great advance of testing equipment and computational capacity.

Generally speaking, differing from those of other underground structures, like tunnel, subway station, and basement, the cross section of utility tunnel is relatively smaller and the tunnel is buried shallowly. In addition, with the development of prefabricated construction techniques, many of utility tunnels are installed section by section, in which case the joint connection is inevitable. Comparing with the utility tunnel without joint connection, it may have some special mechanical and deformation characteristics especially under seismic condition. However, the joint connection was less considered along the longitudinal direction of utility tunnel in current studies, based on Table 1.

With the help of shaking table testing system, the current research studied the seismic behaviors of double-box utility tunnel, especially for seismic performance of the joint connection along the longitudinal direction of utility tunnel by considering two kind of utility tunnel models— with and without joint connection. For simplification, the model without joint connections is named as model I, while the other model with joint connections is model II. To mitigate the boundary effect of soil container during shaking process, a laminar steel soil container was used. The input shaking wave is the seismic spectrum of 1940 El Centro earthquake, which was adjusted to have the peak ground acceleration (PGA) of 0.2g, 0.4g, 0.8g, and 1.2g to examine the effect of PGA on seismic behaviors. Through a series of sensors pre-arranged on the structure and in the soil, such as accelerometers, earth pressure gauges and strain gauges,

Table 1  
Summary of studies on seismic behaviors of under underground structures since 1995.

Structure type	Characteristics of structure	Research method	Country	Reference(s)
Subway station	—	Field investigation	Japan	Iida et al., 1996
Tunnels	Long lined	Analytical method	Greece	Stamos and Beskos, 1996
Subway structure	Dakai subway station model	Shaking table model test	Japan	Iwatate et al., 2000
Buried structure	Rectangular, without joint connection	Developing based on the exiting method	Spain	Gil et al., 2001
Tunnel	Circular	Analytical method, numerical simulation	USA, Korea	Hashash et al., 2005
Duct	Two-box, without joint connection	Analytical method, numerical simulation	Japan	Tateishi, 2005
Utility tunnel	Single-box, without joint connection	shaking table model test, numerical simulation	China	Chen et al., 2010; Chen et al., 2012; Jiang et al., 2010
Subway station	Rectangular and Multistory	shaking table model test, numerical simulation	China	Chen et al., 2013; Chen et al., 2015
Tunnel	Rectangular	centrifuge tests, numerical simulation	Greece and UK	Tsinidis et al., 2015
Tunnel	Long	Shaking table model test	China	Yu et al., 2017
Utility tunnel	Without joint connection	Shaking table model test	China	Chen et al., 2020; Ding et al., 2021
Subway station	Rectangular	Numerical simulation	China	Ma et al., 2018
Tunnel	Shallow buried	Numerical simulation	India, Australia	Patil et al., 2018
Tunnel	Circular	Shaking table model test	China	Wang et al., 2018a
Shield tunnel	Circular	Analytical solutions	China	Yu et al., 2018
Pipeline	Deep buried	Shaking table model test	China	Yan et al., 2018
Utility tunnel	Without joint connection	pseudo-static test	China	Yang et al., 2019b
Subway station	Rectangular and Multistory	Shaking table model test, numerical simulation	China	Zhuang et al., 2019a, 2019b; Chen et al., 2019a
Atriumsubway station	Two-story and zero buried depth	Shaking table model test	China	Zhao et al., 2019

three kinds of seismic responses were measured during the shaking process including the acceleration response, the dynamic earth pressure response and the bending moment response. From different perspectives, several practical conclusions on the seismic behaviors of double-box utility tunnel and its joint connection were obtained.

## 2 Model testing design and instrumentations

### 2.1 Shaking table facility

This study was performed via a shaking table testing system developed by ANCO company in the United States. For shaking table tests, it is important to mitigate the boundary effect, in which case two types of soil containers are generally employed, i.e., laminar soil container (Chen et al., 2015) and rigid soil container with soft material at the inner side of the boundary (Wang et al., 2018a; Tateishi, 2005). In this test, a laminar steel soil container with the dimension of  $0.95 \text{ m} \times 0.85 \text{ m} \times 0.65 \text{ m}$  (length  $\times$  width  $\times$  height) was applied as shown in Fig. 1. A prototype model whose dimension of cross section is  $6.7 \text{ m} \times 4.5 \text{ m}$  was assumed.

### 2.2 Model preparation

This study employed the scaling laws recommended by Iai (1989) to deduce the similarity relationship among the physical quantities using Buckingham  $\pi$  theorem. The maximum vibration acceleration of this testing equipment is  $1.2g$ , and the environment acceleration of this prototype model is  $0.25g$ . Therefore, when the acceleration similitude ratio is 5, the performance of shaking table can be fully utilized. Given the sizes of the rectangular laminar container and according to the similitude law, this study adopted a geometry similitude ratio of 15. The simulation law and similarity ratios about the physical model for the 1-g conditions suggested by Iai (1989) are listed in Table 2.

Figure 2 shows the model making process. It can be seen that the test utility models were made of galvanized iron

wire with the diameter of 2.2 mm (see Figs. 2 (a)) and micro-concrete with measured modulus of 6062 MPa, and the dimension is  $44.67 \text{ cm} \times 30 \text{ cm} \times 80 \text{ cm}$  (width  $\times$  height  $\times$  total length) (see Fig. 2 (d) and (e)). Based on Lee et al. (2012), the distance between the side-wall of model and boundary of soil container is more than  $1/20$  of model width, and hence, the boundary effect can be effectively mitigated. To ensure the formwork (see Fig. 2 (b)) was fully filled with micro-concrete, the formwork was firstly placed upright so that the micro-concrete can be poured into from the end part of the formwork (see Fig. 2 (c)). Simultaneously, the iron bar was used to vibrate the micro-concrete and the hammer was applied to hit the formwork, which further ensure that considerable voids will not exist in the utility tunnel model.

Figure 3 shows the installation of testing system in this test. Firstly, the utility tunnel models need to be prepared well such as the arrangement of strain gauges. Especially for model II, the joint connection should be cautiously treated. The Model II consists of two sections which contact each other directly, and the joint is covered by HDPE black geomembrane with thickness of 0.2 mm (see Fig. 3 (b)), whose detailed diagram is shown in Fig. 3(c). Therefore, this joint connection can be regarded as a kind of highly flexible connection. Actually, there is a variety of joint types with the flexibility ranging from very low to very high. When the flexibility of joints becomes low, the behavior of the utility tunnel becomes the one without joints. Thus, the test of the utility tunnel with high flexibility was conducted, to better compare its seismic behavior with the one without joints and clearly demonstrate the effect of the joints. The influence of the other types of joints should be between these two bounds.

The test ground was simulated by dry standard sand from Xiamen, China with the layered tamping treatment. And the particle size distribution is shown in Fig. 4, and the cohesion stress  $c$  and friction angle  $\varphi$  is 0 and  $40^\circ$ , respectively. During filling process of the standard sand, the utility tunnel model and some sensors (like earth pressure gauges and accelerometers) were installed at the pre-determined location of the soil container. Lastly, installation of testing system was finished, and the simulated sand field density approximately equals to  $1740 \text{ kg/m}^3$ .

### 2.3 Testing program

The seismic spectrum of 1940 El Centro earthquake is widely used in the earthquake engineering research. In this test, it was also considered as the input, as shown in Fig. 5. Specially, it was adjusted to have PGA of  $0.2g$ ,  $0.4g$ ,  $0.8g$ , and  $1.2g$  respectively to exam the effect of PGA, and the time was compressed based on the similarity ratios. Therefore, based on the given acceleration similarity ratio of 5:1, the input PGA will be less than  $0.4g$  for the actual project. The vibration was exerted at the base of shaking table system in the uniaxial direction perpendicular to the longitudinal direction of utility tunnel model as shown in Fig. 3.

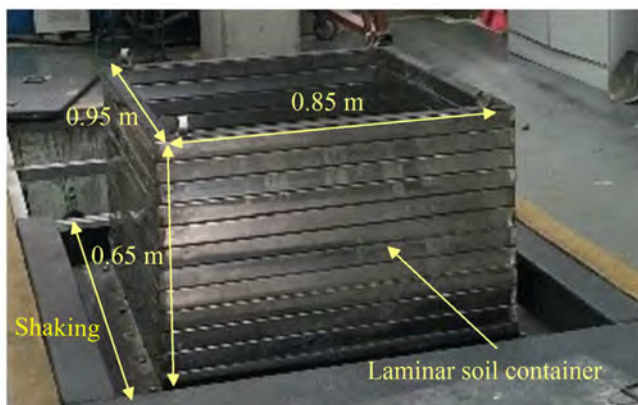


Fig. 1. Shaking table system.

Table 2  
Similarity ratios for some parameters.

Parameter	Determination	Similarity ratio
Geometry $S_l$	Selected	1:15
Strain $S_\epsilon$	Selected	1:1
Stress $S_\sigma$	Selected	1:3
Elastic modulus $S_E$	$S_E = S_\sigma / S_\epsilon$	1:3
Acceleration $S_a$	Selected	5:1
Density $S_\rho$	$S_\rho = S_E / (S_l S_a)$	1:1
Time $S_t$	$S_t = (S_l / S_a)^{1/2}$	1:8.67
Reinforcement	Keep the reinforcement ratio consistent with the actual project	

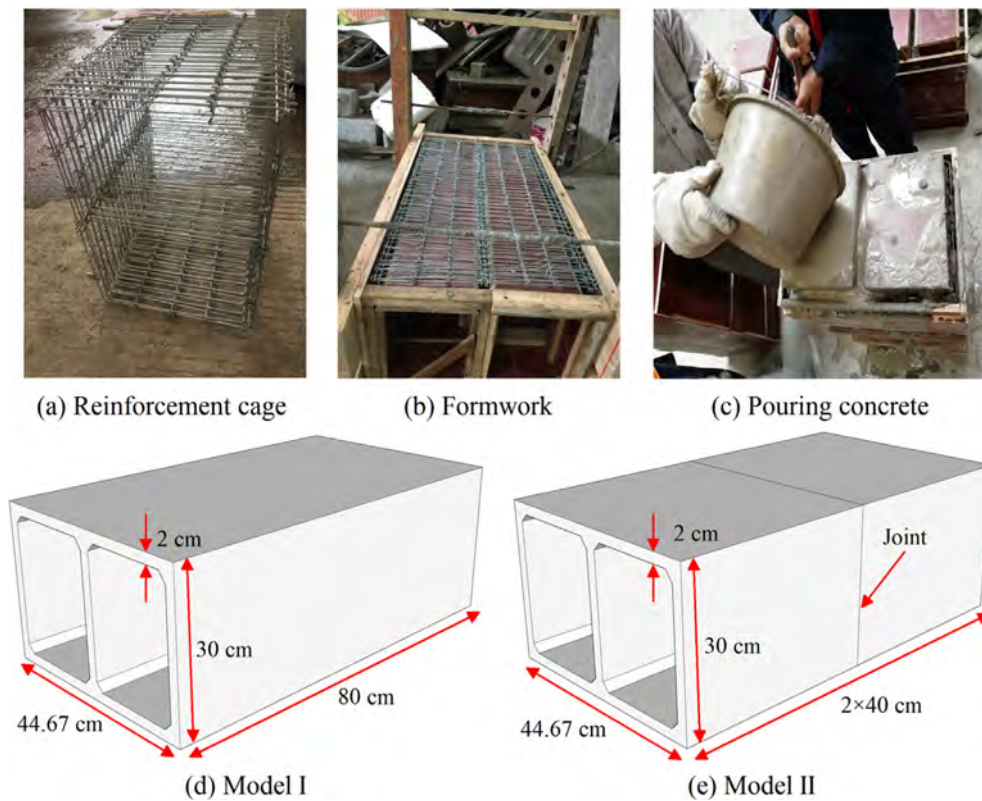


Fig. 2. Model making process.

#### 2.4 Instrumentation scheme

In this test, there are mainly three responses which are of concern, including the earth pressure response of testing ground, acceleration response of structure and the surrounding soil and strain responses of structure, which can be monitored by earth pressure gauges (denoted by “P”), accelerometers (denoted by “A”) and strain gauges (denoted by “S”) as shown in Figs. 6 and 7. Figure 6 shows the vertical view of sensor layout and Fig. 7 plots the sectional view of sensor layout for model I and II.

For model I, the earth pressure gauges, accelerometers and strain gauges were set at the middle cross section of the model. For model II, these sensors were set at the cross section of joint connection to investigate the effect of joint connections by comparing the testing results obtained from model I. After setting the sensors above, the testing data

was obtained by the data collecting instrument-DH5921 developed by Donghua company. To eliminate the influence of different initial value of every sensor, the measuring value was reset before conducting a new test. Hence, the testing data obtained from every test was the incremental data. For earth pressure and strain response, if the value is positive, it suggests that this physical magnitude increases. Apparently, the resetting procedure had no influence on the work of accelerometer.

### 3 Testing result analysis and discussion

#### 3.1 Dynamic earth pressure response

Figure 8 shows the maximum earth pressure distribution along depth, extracted from the measuring points—P1, P2, P3, P4, P5, P6 and P7. Apparently, the dynamic earth

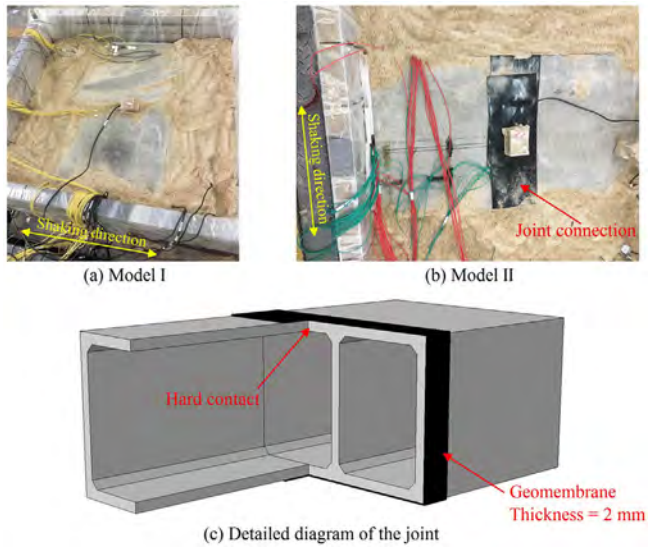


Fig. 3. Installation of testing model.

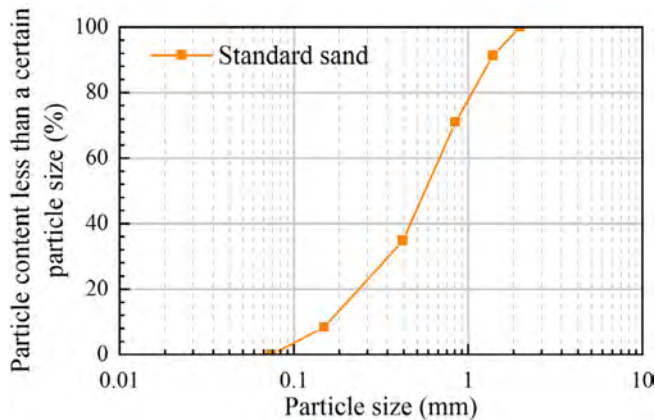


Fig. 4. Particle size distribution of standard sand in Xiamen.

pressure responds more dramatic in the depth range of utility tunnel model than those in other depth ranges. Based on the works of Tsinidis (2017), Tsinidis et al. (2016a) and Tsinidis et al. (2016b), the phenomenon above can be attributed to the soil-structure relative stiffness. Particularly, the maximum dynamic earth pressure has an approximate distribution of inverted “W” for both two models, and this kind of distribution characteristic of dynamic earth pressure was also reported by Chen et al. (2013), which can be explained by the rocking-racking responses. Under the horizontal seismic excitation, the rocking-racking responses may exist for rectangular tunnel-like structure (Tsinidis 2017; Tsinidis et al., 2016a). More specifically, the rectangular tunnel-like structure tends to rotate around the geometrical centroid of the section, and even if the center of rotation does not coincide with the centroid, these two points are very close to each other (Tsinidis 2017). Therefore, the displacement in the midpoint of the side-wall is smaller compared with those at the top and bottom of the side-wall, and as a result, the

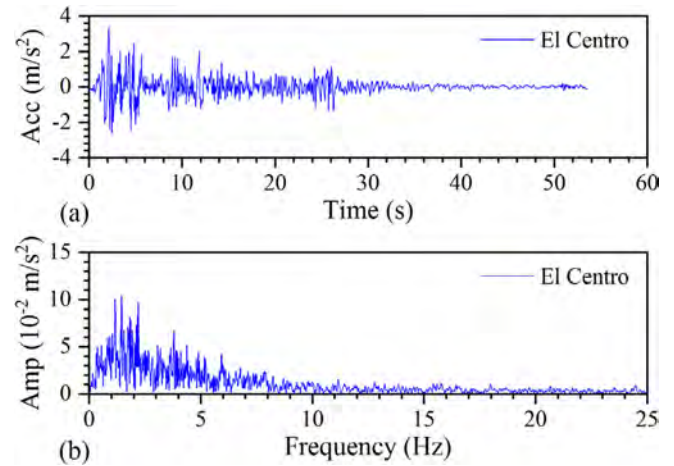


Fig. 5. (a) Acceleration time history, and (b) Fourier spectrum of El Centro earthquake.

interacting force between wall and soil (the earth pressure) in the midpoint is also smaller. Accordingly, the distribution characteristic of inverted “W” occurs due to the mechanism above.

In addition, there are two responses different between models I and II. Firstly, the magnitude of dynamic earth pressure of model I is generally greater than that of model II; secondly, the difference of the maximum dynamic earth pressure at the top, middle and bottom part of the side-wall is rather significant for model I, while the difference of model II becomes less evident. These two points above can be explained by the reduction of structure integrity or the reduction of soil-structure relative stiffness along the longitudinal direction. Apparently, the reduction of stiffness means the increase in the structure flexibility, and hence, model II is more likely to follow the kinematical mechanism of ground under shaking than model I, so that the dynamic earth pressure correspondingly becomes more uniform at the top, middle and bottom parts of model.

Since the dynamic earth pressure responses at measuring points P3, P4 and P5 are relatively more significant, the earth pressure time histories at these measuring points are plotted in Figs. 9 and 10 for model I and II, respectively. For brevity, the earth pressure time histories of the remaining measuring points are shown in Figs. A1 and A2 in the appendix. From Fig. 9, the dynamic earth pressure at the measuring point-P4 is generally less than the values at P3 and P5 during the shaking process, which further demonstrates the distribution characteristic of inverted “W” of dynamic earth pressure. At the end of earthquake, the earth pressure does not restore to the static state and is even less than 0, indicating that the soil adjacent to the side-wall may become looser after an earthquake. According to Fig. 10, when the earthquake occurs, the dynamic earth pressure at the measuring point P4 generally is not smaller than those at P3 and P5. The phenomenon above reflects that at the beginning of shaking process, model II tends to follow the motion of ground due to the existence

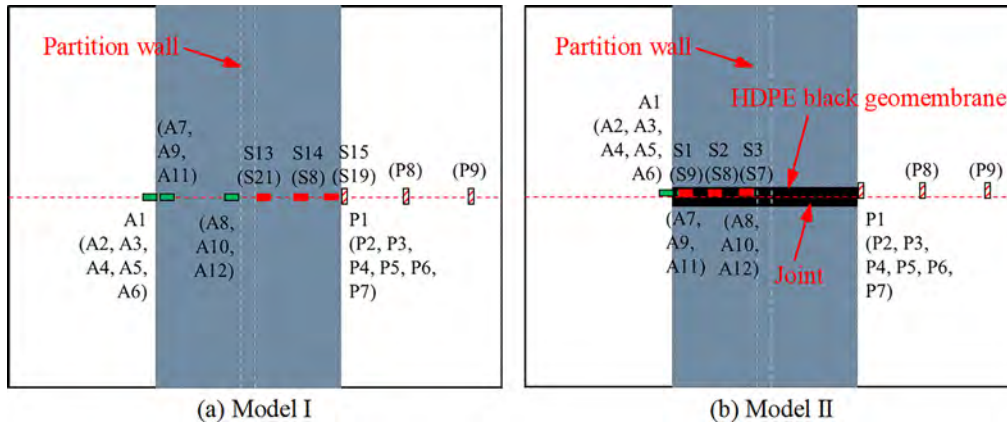
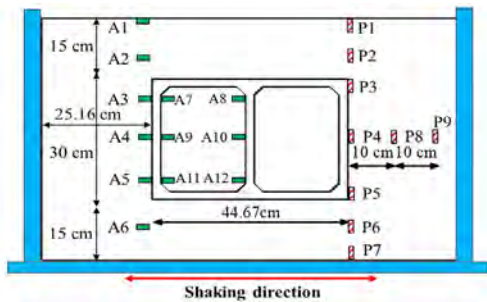
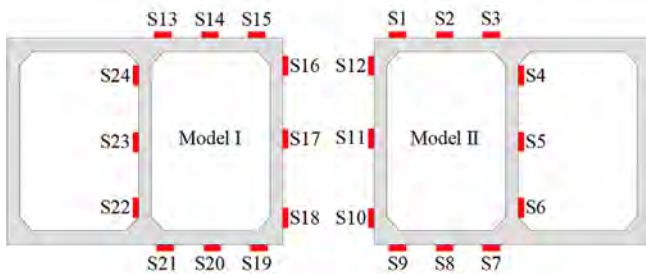


Fig. 6. Vertical view of sensor layout for model I and II.



(a) Earth pressure gauges and accelerometers



(b) Strain gauges

Fig. 7. Sectional view of sensor layout for model I and II.

of joint connections, especially under the relatively lower input PGA. Nevertheless, the dynamic earth pressure at the measuring point P4 is still less than those at the P3 and P5 in the sequent shaking process, indicating that the existing of the joint connections mainly make the magnitude of dynamic earth pressure decrease, but has less considerable effects on the distribution characteristic of dynamic earth pressure along the depth. Similarly, the earth pressure field may not restore to static state, especially at the middle part of the side-wall, and this result is consistent with that by Tsinidis et al. (2015), but more evident than that of model I.

### 3.2 Acceleration response

Figure 11 shows the distribution of maximum acceleration response and the amplification factor along depth in the soil near by the side-wall for both models, in which the distribution of model II is given in dash line, and the distribution of model I is depicted as solid line. These two model systems have the similar distribution pattern: decreasing with depth on the whole and the similar magnitude of response. From this aspect, if the underground structure was constructed at a shallower buried depth, the structure will be more vulnerable. This conclusion is basically in agreement with previous researches

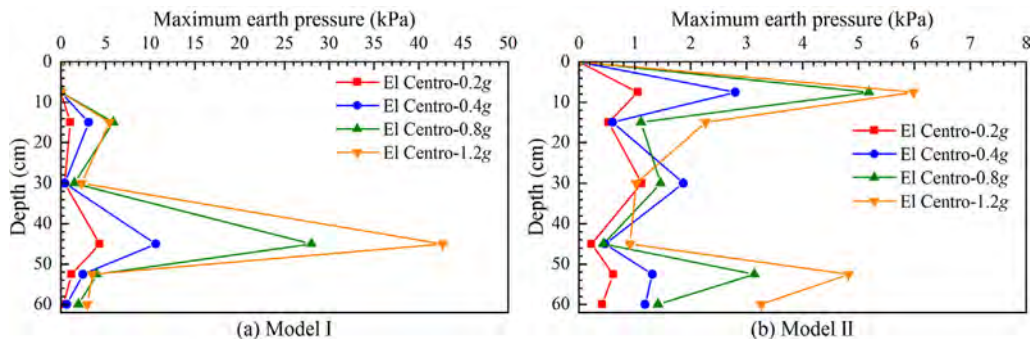


Fig. 8. Maximum earth pressure distribution along depth.

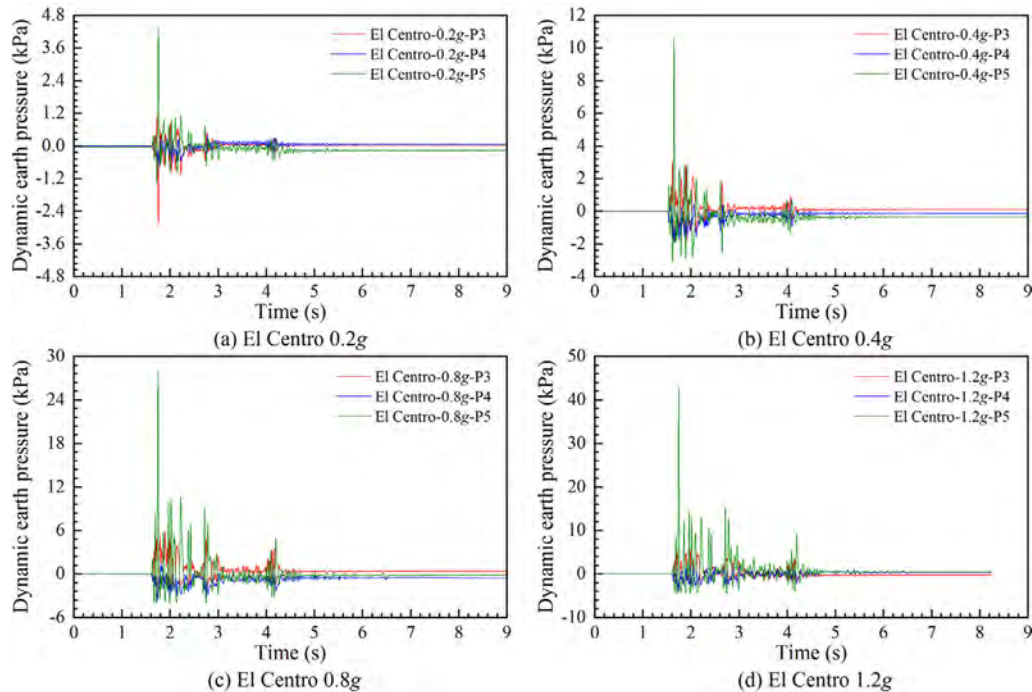


Fig. 9. Earth pressure time history of the surrounding soil neighboring the side-wall of model I.

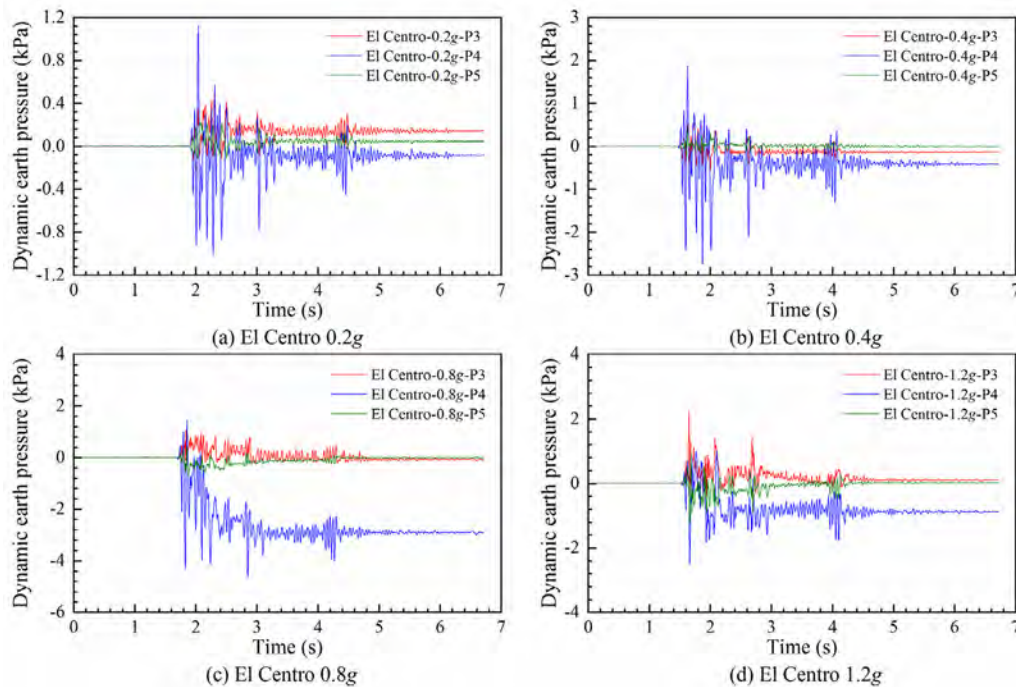


Fig. 10. Earth pressure time history of the surrounding soil neighboring the side-wall of model II.

(Chen et al., 2013; Tsinidis et al., 2015; Zhao et al., 2019). However, they did not consider the effect of input PGA on the acceleration response. When the input PGA is relatively small, like 0.2g in this test, the difference is less significant (see Fig. 11 (a)). When the input PGA is 0.4g and 0.8g, the response of model II is generally less than that of model I, while it is opposite under input PGA of 1.2g

(see Fig. 11 (a)). These two distributions both show that the effect of soil-structure interaction gets more remarkable as input PGA increases, causing the maximum acceleration to decrease to a minimum value and then continue to increase after a reversal point along depth (see Fig. 11 (b)).

Another interesting finding is that the amplification factor of acceleration will decrease with the increase of input

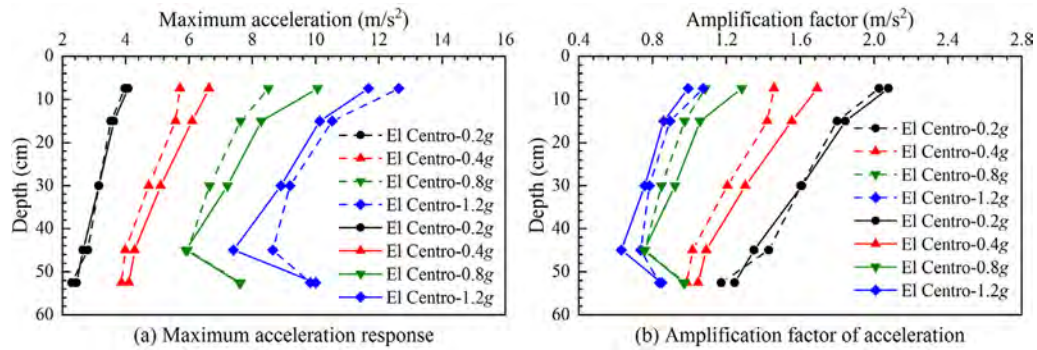


Fig. 11. Distribution of maximum acceleration and amplification factor along depth.

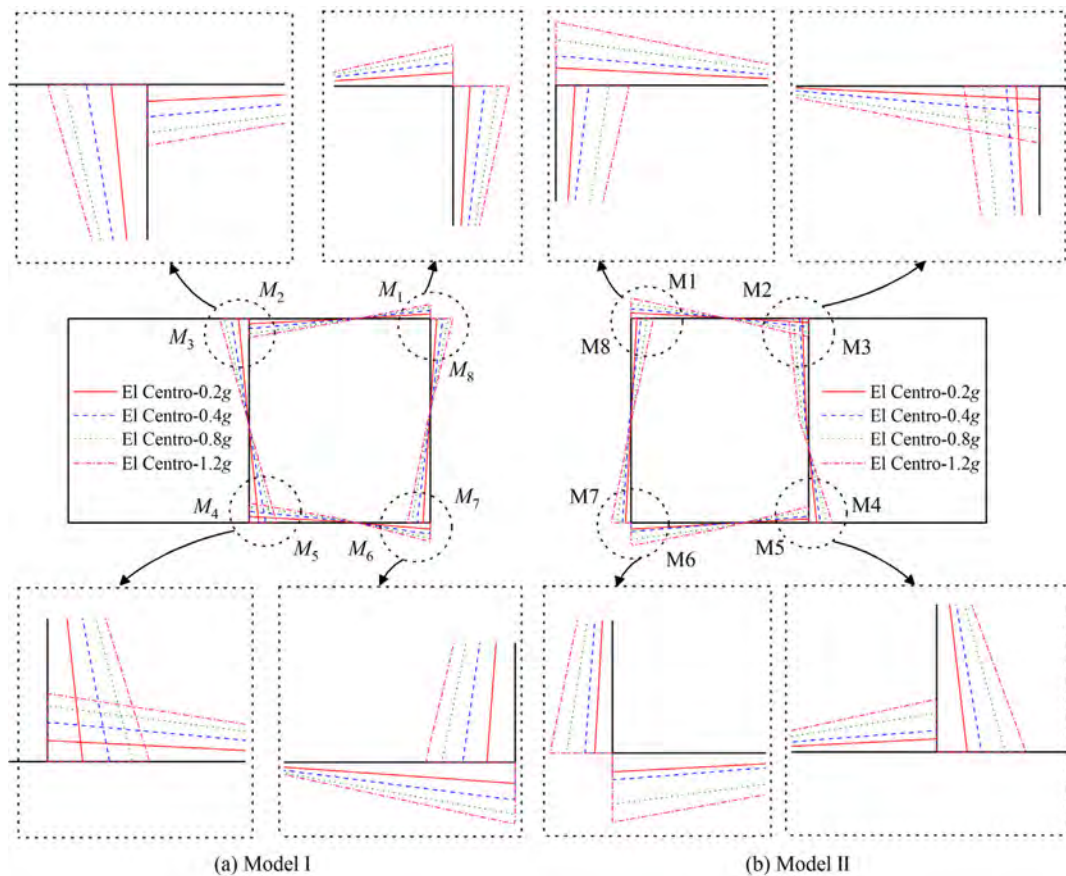


Fig. 12. Bending moment response.

PGA, which may be due to the effect of dynamic property of soil (see Fig. 11 (b)). For example, the greater input PGA will cause greater dynamic shearing strain  $\gamma$ , and  $\gamma$  may lead to the greater damping ratio, which may absorb more energy during the shaking process so that the acceleration response will be mitigated.

In actual project, the utility tunnel will be divided into several cabins based on their function (Yang et al., 2019a). In this test, the two-box utility tunnel model was considered. According the failure modes of Dakai subway station in 1995 (Iida et al., 1996) and the test results of

Chen et al. (2019a), the partition wall may be the vulnerable part under seismic condition. Therefore, three accelerometers (A8, A10, and A12) were arranged at the partition wall corresponding to the three ones (A7, A9, and A11) on the side-wall of model I.

The acceleration time history and Fourier spectrum of side-wall and partition wall for models I and II under different input PGAs are shown in Figs. A3 and A4 in the appendix. From Fig. A3, it can be seen that there is little difference in the acceleration response between the side-wall and the partition wall at the same depth, and these

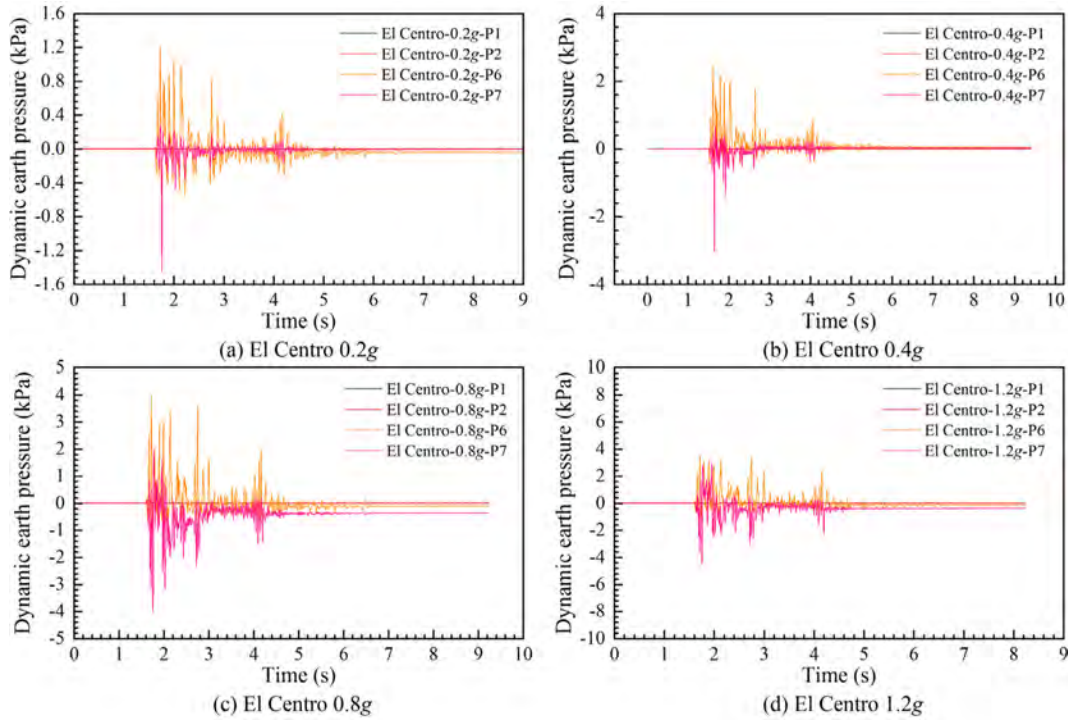


Fig. A1. Earth pressure time history of the surrounding soil neighboring the side-wall of model I.

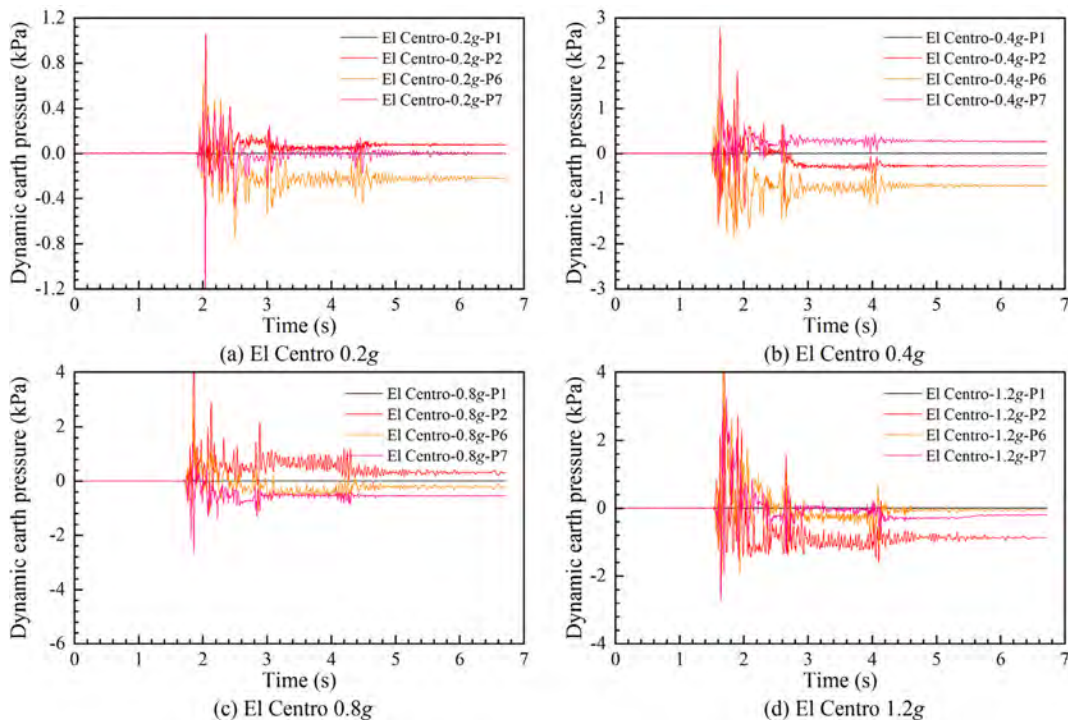


Fig. A2. Earth pressure time history of the surrounding soil neighboring the side-wall of model II.

two parts all show that the acceleration response will increase with input PGA and decrease with depth. Thus, it can be inferred that the damage of partition wall may result from the difference of kinetic response along depth, especially at the top and bottom node of the partition

wall. In addition, the partition wall is a continuous structure so that it has greater stiffness and integrity than the central pillar of Dakai subway station (Iida et al., 1996). Therefore, comparing with those subway stations, the effect of seismic excitation on partition wall is less

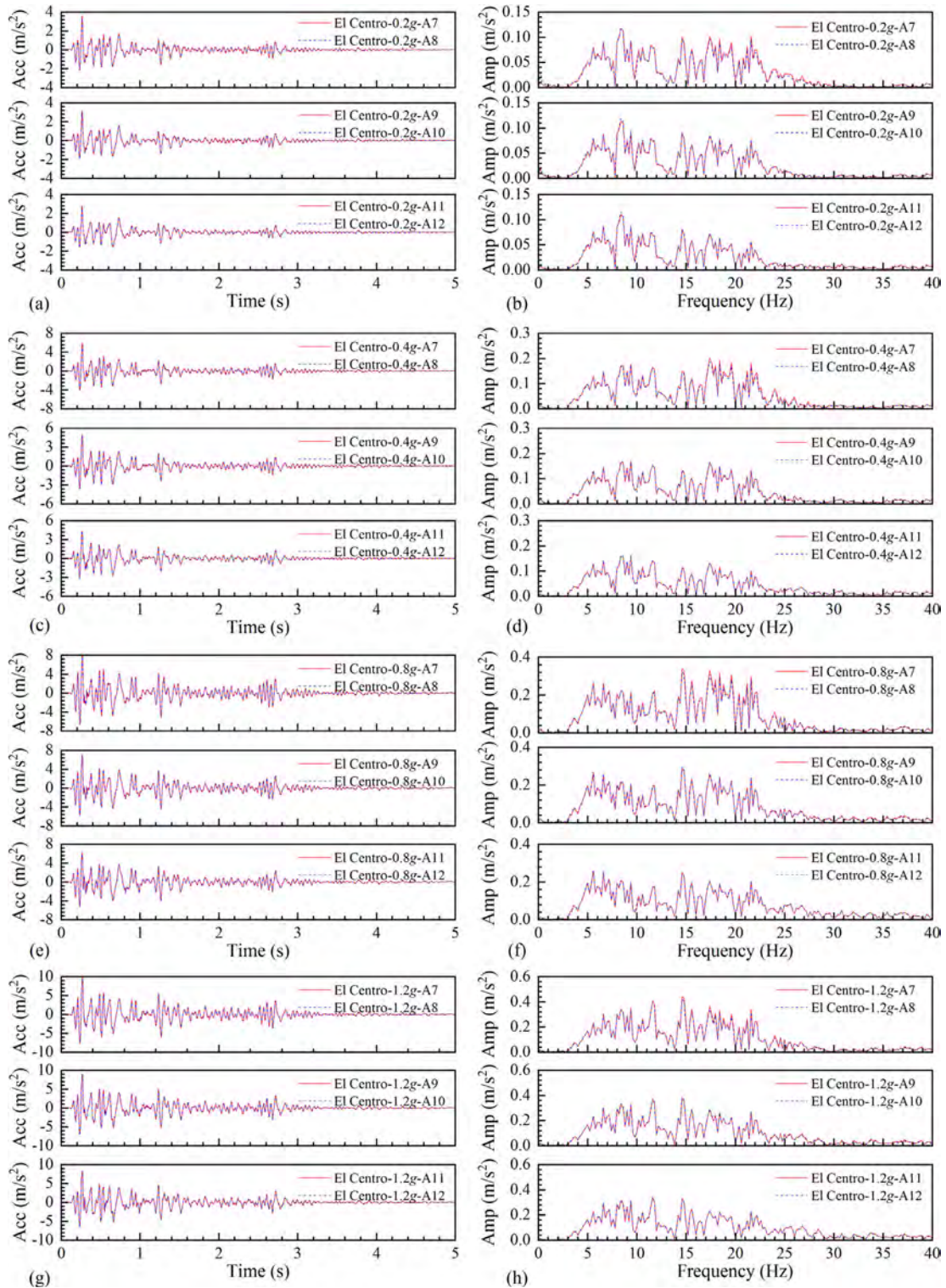


Fig. A3. Acceleration time history and Fourier spectrum of side-wall and partition wall for model I for (a)–(b) 0.2g, (c)–(d) 0.4g, (e)–(f) 0.8g, and (g)–(h) 1.2g.

significant. In Fig. A4, the accelerometer A7 was broken after the test under the input PGA of 0.4g during the testing process. Apparently, the changing pattern and the response magnitude of acceleration time history and

Fourier spectrum are similar with those of model I, indicating that the effect of the flexible joint connection on acceleration response of underground structure is not evident.

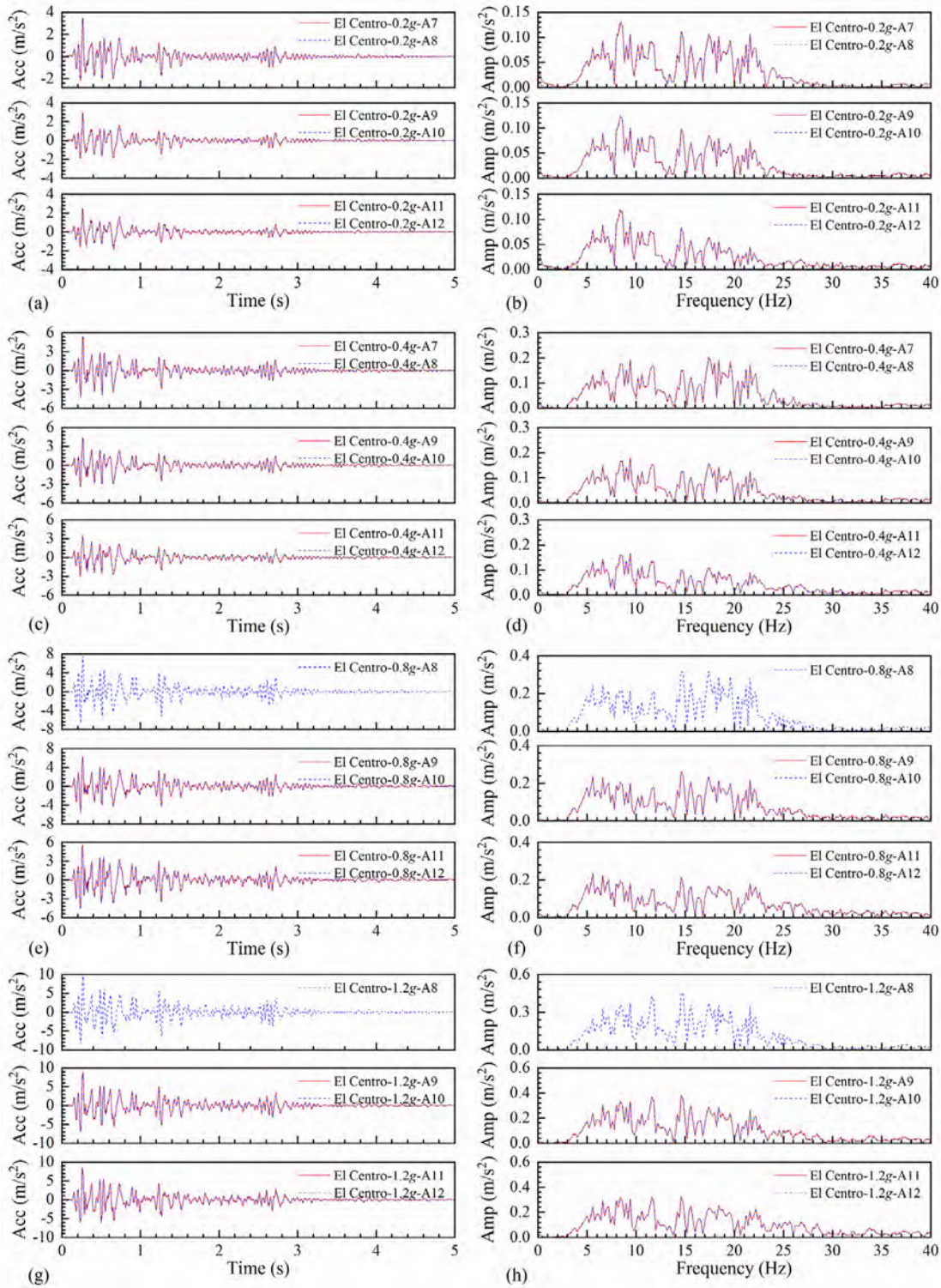


Fig. A4. Acceleration time history and Fourier spectrum of side-wall and partition wall for model II for (a)–(b) 0.2 g, (c)–(d) 0.4g, (e)–(f) 0.8g, and (g)–(h) 1.2g.

### 3.3 Bending moment response

Based on the strain gauges, the strain response can be obtained and used to calculate the bending moment response of structure. Firstly, the time of largest strain

response would be determined, and then the strain responses of all measuring points at that time were extracted to calculate the bending moment using the Eq. (1):

$$M = \varepsilon \cdot W \cdot E \cdot 10^{-9} \quad (1)$$

Table 3  
Corresponding relationship for the measuring points between models I and II.

New name	Model I	Model II	New name	Model I	Model II
M <sub>1</sub>	S15	S1	M <sub>5</sub>	S21	S7
M <sub>2</sub>	S13	S3	M <sub>6</sub>	S19	S9
M <sub>3</sub>	S24	S4	M <sub>7</sub>	S18	S10
M <sub>4</sub>	S22	S6	M <sub>8</sub>	S16	S12

Table 4  
Bending moment value of structure corners for models I and II.

Measuring point	El Centro 0.2g		El Centro 0.4g		El Centro 0.8g		El Centro 1.2 g	
	model I	model II	model I	model II	model I	model II	model I	model II
M <sub>1</sub>	7.08	5.41	12.39	11.21	17.02	20.26	21.21	23.93
M <sub>2</sub>	-7.59	-3.90	-14.76	-9.92	-22.11	-20.34	-27.88	-22.69
M <sub>3</sub>	-13.17	-5.12	-22.26	-9.78	-30.32	-18.85	-36.33	-21.91
M <sub>4</sub>	11.71	7.53	20.56	13.81	28.25	23.63	33.85	27.75
M <sub>5</sub>	9.00	4.35	16.80	8.28	23.70	16.04	29.03	18.66
M <sub>6</sub>	-9.39	-6.58	-16.84	-12.12	-23.08	-23.95	-27.53	-28.96
M <sub>7</sub>	-8.78	-4.91	-16.29	-9.23	-22.74	-17.08	-27.84	-20.05
M <sub>8</sub>	8.22	5.21	15.57	10.37	22.38	19.18	27.66	22.67

Where,  $M$  is the bending moment of structure per unit length,  $N\cdot m/m$ ;  $\varepsilon$  is the strain response,  $10^{-6}$ ;  $W$  is the section modulus in bending,  $mm^3$ ; and  $E$  is the elastic modulus of the micro-concrete, MPa.

Figure 12 shows the distribution of additional bending moment response, where the bending moment causing tensile stress on the outside of sidewall is positive, and vice versa. Based on Fig. 12, the greater additional bending moment response will develop at the structure corners for both models I and II. Hence, the safety of structure at the corners should be paid more attention, which is consistent with the results of Chen et al. (2019a) when the ground surface is level. Since seismic loading is kind of reciprocating loading, the bending moment response for models I and II can be compared by the means of Table 3 and the measuring points were renamed as  $M_i$  ( $i$  is the number of structure corners).

Table 4 shows the specific value of additional bending moment at the structure corners. It can be seen that the bending moment response of model I is generally greater than that of model II at the same measuring point under the same input PGA except for the highlighted value. It means that the structural integrity decreases due to the existence of joint connections, which leads to the relatively slight response to the structure. Other seismic responses, such as earth pressure response also confirm this finding. Because of this, applying the joint connections appropriately into the construction of utility tunnel could mitigate the seismic damage to the underground structure under earthquake. Last but not the least, as pre-mentioned, it is the additional bending moment response rather than the absolute bending moment response that was taken into consideration, which means that the location where the additional bending moment is

larger may be not more vulnerable, which depends on the initial bending moment in the structure subjected to the initial stress field and the structure design (e.g., Tsinidis et al., 2015).

#### 4 Conclusions

Based on the shaking table tests, this paper studied the seismic behaviors of double box utility tunnel without or with joint connections. Through analyzing the earth pressure response, acceleration response, and bending moment response under seismic condition, several conclusions are obtained as follows:

(1) The maximum earth pressure has a distribution of inverted “W” for utility tunnels without or with joint connections. The existing of the joint connections mainly affects the magnitude of dynamic earth pressure and has relatively less impacts on the distribution of dynamic earth pressure along the depth.

(2) When the input PGA is relatively small such as 0.2g, the difference of maximum acceleration distribution is not remarkable.

(3) Side-wall and partition wall have the consistent acceleration time history and Fourier spectrum for both utility tunnels without and with joint connections. Effect of joint connections on acceleration is not evident.

(4) Greater additional bending moment develops at the structure corners for both two kinds of models, and the existence of joint connections will mitigate the additional bending moment response on the structures under seismic condition.

(5) In actual project, the joint connections should be appropriately considered to mitigate the seismic damage to utility tunnels.

Although the conclusions obtained in this study are based on a double-box utility tunnel, it can still be generalized to the utility tunnels with other cross-sections such as the single-box utility tunnel (Ding et al., (2020)). In addition, the test of the utility tunnel with high flexibility was conducted to better compare its seismic behavior with the one without joints and clearly demonstrate the effect of the joints. The influence of the other types of joints should be between these two bounds.

### Declaration of Competing Interest

The authors declare that they have no known competing financial interests or personal relationships that could have appeared to influence the work reported in this paper.

### Acknowledgements

The project was supported by Natural Science Foundation of China (Grant Nos. 52078086 and 51778092) Innovation Group Science Foundation of the Natural Science Foundation of Chongqing, China (Grant No. cstc2020jcyj-cxttX0003) State Education Ministry and the Fundamental Research Funds for the Central Universities (2019 CDJSK 04 XK23). The authors would also like to sincerely thank the anonymous reviewers for their insightful comments and suggestions.

**Appendix** This appendix includes the earth pressure time history of the surrounding soil neighboring the side-wall and acceleration time history and Fourier spectrum of side-wall and partition wall for model I and II.

### References

- Chen, G. X., Wang, Z., Zuo, X., Du, X. L., & Gao, H. (2013). Shaking table test on the seismic failure characteristics of a subway station structure on liquefiable ground. *Earthquake Engineering & Structural Dynamics*, 42(10), 1489–1507.
- Chen, G. X., Chen, S., Zuo, X., Du, X. L., Qi, C. Z., & Wang, Z. H. (2015). Shaking-table tests and numerical simulations on a subway structure in soft soil. *Soil Dynamics and Earthquake Engineering*, 76, 13–28.
- Chen, J., Jiang, L. Z., Li, J., & Shi, X. J. (2012). Numerical simulation of shaking table test on utility tunnel under non-uniform earthquake excitation. *Tunnelling and Underground Space Technology*, 30, 205–216.
- Chen, J., Shi, X. J., & Li, J. (2010). Shaking table test of utility tunnel under non-uniform earthquake wave excitation. *Soil Dynamics and Earthquake Engineering*, 30(11), 1400–1416.
- Chen, S., Wang, X., Zhuang, H., Xu, C., & Zhao, K. (2019a). Seismic response and damage of underground subway station in a slightly sloping liquefiable site. *Bulletin of Earthquake Engineering*, 17(11), 5963–5985.
- Chen, Z. X., Yang, P., Liu, H. L., Zhang, W. G., & Wu, C. Z. (2019b). Characteristics analysis of granular landslide using shaking table model test. *Soil Dynamics and Earthquake Engineering*, 126, 105761.
- Chen, X., Ma, B., Najafi, M., & Zhang, P. (2021). Long rectangular box jacking project: A case study. *Underground Space*, 6(2), 101–125.
- Chen, Z., Liang, S., & He, C. (2020). Effects of different coherency models on utility tunnel through shaking table test. *Journal of Earthquake Engineering*, 24, 579–600.
- Davis, C. A., Lee, V. W., & Bardet, J. P. (2001). Transverse response of underground cavities and pipes to incident SV waves. *Earthquake Engineering & Structural Dynamics*, 30(3), 383–410.
- Ding, X., Feng, L., Wang, C., Chen, Z., & Han, L. (2020). Shaking table tests of the seismic response of a utility tunnel with a joint connection. *Soil Dynamics and Earthquake Engineering*, 133, 106133.
- Ding, X. M., Zhang, Y. L., Wu, Q., Chen, Z. X., & Wang, C. L. (2021). Shaking table tests on the seismic responses of underground structures in coral sand. *Tunnelling and Underground Space Technology*, 109, 103775.
- Gil, L. M., Hernandez, E., & De la Fuente, P. (2001). Simplified transverse seismic analysis of buried structures. *Soil Dynamics and Earthquake Engineering*, 21(8), 735–740.
- Hashash, Y. M. A., Park, D., & Yao, J. I. C. (2005). Ovaling deformations of circular tunnels under seismic loading, an update on seismic design and analysis of underground structures. *Tunnelling and Underground Space Technology*, 20(5), 435–441.
- Huang, J., Wang, G., & Wang, J. (2018). Settlement Control, Monitoring and Analysis of Utility Tunnel on Soft Soil Foundation. *Chinese Journal of Underground Space and Engineering*, 14, 845–859 (in Chinese).
- Iai, S. (1989). Similitude for shaking table tests on soil-structure-fluid model in 1g gravitational field. *Soils and Foundations*, 29(1), 105–118.
- Iida, H., Hiroto, T., Yoshida, N., & Iwafuji, M. (1996). Damage to Daikai subway station. *Soils and Foundations*, 36, 283–300.
- Iwatate, T., Kobayashi, Y., Kusu, H., & Rin, K. (2000). Investigation and Shaking Table Tests of Subway Structures of the Hyogoken-Nanbu Earthquake. In 12th World Conference on Earthquake Engineering, January 30 to February 4, 2000; Auckland, New Zealand.
- Jiang, L., Chen, J., & Li, J. (2010). Seismic response of underground utility tunnels: Shaking table testing and FEM analysis. *Earthquake Engineering and Engineering Vibration*, 9(4), 555–567.
- Lee, C. J., Wei, Y. C., & Kuo, Y. C. (2012). Boundary effects of a laminar container in centrifuge shaking table tests. *Soil Dynamics and Earthquake Engineering*, 34(1), 37–51.
- Li, T., Liu, L., Li, J. Q., & Yin, M. (2019). Economic Analysis for Installation of Electrical Cables into Utility Tunnels in China. In Iccmb 2019 – the 2nd International Conference on Computers in Management and Business. March 24–27, 2019. Cambridge, United Kingdom. New York: ACM Press 2019.
- Ma, C., Lu, D. C., Du, X. L., & Qi, C. (2018). Effect of buried depth on seismic response of rectangular underground structures considering the influence of ground loss. *Soil Dynamics and Earthquake Engineering*, 106, 278–297.
- Paolucci, R., & Smerzini, C. (2018). Empirical evaluation of peak ground velocity and displacement as a function of elastic spectral ordinates for design. *Earthquake Engineering & Structural Dynamics*, 47(1), 245–255.
- Patil, M., Choudhury, D., Ranjith, P. G., & Zhao, J. (2018). Behavior of shallow tunnel in soft soil under seismic conditions. *Tunnelling and Underground Space Technology*, 82, 30–38.
- Sakai, H., Pulido, N., Hasegawa, K., & Kuwata, Y. (2017). A new approach for estimating seismic damage of buried water supply pipelines. *Earthquake Engineering & Structural Dynamics*, 46(9), 1531–1548.
- Stamos, A. A., & Beskos, D. E. (1996). 3-D seismic response analysis of long lined tunnels in half-space. *Soil Dynamics and Earthquake Engineering*, 15(2), 111–118.
- Tan, Y., Lu, Y., & Wang, D. L. (2019). Practical Solutions for Concurrent Excavation of Neighboring Mega Basements Closely Surrounded by Utility Tunnels in Shanghai Hongqiao CBD. *Practice Periodical on Structural Design and Construction*, 24(4), 05019005.
- Tateishi, A. (2005). A study on seismic analysis methods in the cross section of underground structures using static finite element method. *Structural Engineering Earthquake Engineering*, 22(1), 41s–54s.
- Tsinidis, G. (2017). Response characteristics of rectangular tunnels in soft soil subjected to transversal ground shaking. *Tunnelling and Underground Space Technology*, 62, 1–22.
- Tsinidis, G., Pitilakis, K., & Madabhushi, G. (2016a). On the dynamic response of square tunnels in sand. *Engineering Structures*, 125, 419–437.
- Tsinidis, G., Rovithis, E., Pitilakis, K., & Chazelas, J. L. (2016b). Seismic response of box-type tunnels in soft soil: Experimental and numerical investigation. *Tunnelling and Underground Space Technology*, 59, 199–214.

- Tsinidis, G., Pitilakis, K., Madabhushi, G., & Heron, C. (2015). Dynamic response of flexible square tunnels: Centrifuge testing and validation of existing design methodologies. *Géotechnique*, 65(5), 401–417.
- Valdenebro, J. V., & Gimena, F. N. (2018). Urban utility tunnels as a long-term solution for the sustainable revitalization of historic centres: The case study of Pamplona-Spain. *Tunnelling and Underground Space Technology*, 81, 228–236.
- Valdenebro, J. V., Gimena, F. N., & Lopez, J. J. (2019). Construction process for the implementation of urban utility tunnels in historic centres. *Tunnelling and Underground Space Technology*, 89, 38–49.
- Von der Tann, L., Sterling, R., Zhou, Y., & Metje, N. (2020). Systems approaches to urban underground space planning and management – A review. *Underground Space*, 5(2), 144–166.
- Wang, G., Yuan, M., Miao, Y., Wu, J., & Wang, Y. (2018a). Experimental study on seismic response of underground tunnel-soil-surface structure interaction system. *Tunnelling and Underground Space Technology*, 76, 145–159.
- Wang, T., Tan, L., Xie, S., & Ma, B. (2018b). Development and applications of common utility tunnels in China. *Tunnelling and Underground Space Technology*, 76, 92–106.
- Xu, X., Ma, J. X., & Ma, H. M. (2018). Influence of burial depth on Soil Arch in Utility Tunnel. In *IOP Conference Series: Earth and Environmental Science*, 153 052037.
- Yang, C., Peng, F. L., Xu, K., & Zheng, L. N. (2019a). Feasibility study on the geothermal utility tunnel system. *Sustainable Cities and Society*, 46 101445.
- Yang, Y. M., Tian, X. R., Liu, Q. H., Zhi, J. B., & Wang, B. (2019b). Anti-seismic behavior of composite precast utility tunnels based on pseudo-static tests. *Earthquakes and Structures*, 17(2), 233–244.
- Yan, K., Zhang, J., Wang, Z., Liao, W., & Wu, Z. (2018). Seismic responses of deep buried pipeline under non-uniform excitations from large scale shaking table test. *Soil Dynamics and Earthquake Engineering*, 113, 180–192.
- Yu, H., Yan, X., Bobet, A., Yuan, Y., Xu, G., & Su, Q. (2017). Multi-point shaking table test of a long tunnel subjected to non-uniform seismic loadings. *Bulletin of Earthquake Engineering*, 16(2), 1041–1059.
- Yu, H., Zhang, Z., Chen, J., Bobet, A., Zhao, M., & Yuan, Y. (2018). Analytical solution for longitudinal seismic response of tunnel liners with sharp stiffness transition. *Tunnelling and Underground Space Technology*, 77, 103–114.
- Zhang, W. G., Han, L., Feng, L., Wang, L., Liu, H. L., Ding, X. M., ... Aljarmouzi, A. (2020). Study on seismic behaviors of a double box utility tunnel with joint connections using shaking table model tests. *Soil Dynamics and Earthquake Engineering*, 136 106118.
- Zhao, H., Yuan, Y., Ye, Z., Yu, H., & Zhang, Z. (2019). Response characteristics of an atrium subway station subjected to bidirectional ground shaking. *Soil Dynamics and Earthquake Engineering*, 125 105737.
- Zhuang, H. Y., Wang, R., Shi, P., & Chen, G. (2019a). Seismic response and damage analysis of underground structures considering the effect of concrete diaphragm wall. *Soil Dynamics and Earthquake Engineering*, 116, 278–288.
- Zhuang, H. Y., Wang, X., Miao, Y., Yao, E., Chen, S., Ruan, B., & Chen, G. (2019b). Seismic responses of a subway station and tunnel in a slightly inclined liquefiable ground through shaking table test. *Soil Dynamics and Earthquake Engineering*, 116, 371–385.
- Zhu, H., Huang, X., Li, X., Zhang, L., & Liu, X. (2016). Evaluation of urban underground space resources using digitalization technologies. *Underground Space*, 1(2), 124–136.